iRIC Easy-performable Long-wave Inundation MOdel (ELIMO)* Users Guide

Ver. 4.0

June 26, 2023

Introduction

The 2011 Tohoku earthquake tsunami brought great damages to human lives, industries and economics in Japan, and provided an important lesson for disaster reduction and evacuation. We have reconsidered the disaster prevention policy and tried to renew multilateral regional disaster plans for multiple scenarios of tsunami onsets. The estimation of regional tsunami heights provide fundamental conditions to design the disaster plans; developing infrastructures, hazard maps and managing evacuation for various scenarios. While reasonable tsunami computation to predict the tsunami heights along coasts need to be performed, it requires technical knowledge and experiences to operate computer simulators as well as expensive high-performance computers. Whereas local government needs to make the local disaster and evacuation plans to save the local resident against tsunamis, it may be difficult for them to predict the heights by themselves because the absence of human and computer resources, which may slow down procedures of planning.

iRIC-ELIMO has been developed with a motto of "simple and easy tsunami computation" for people with minimum knowledge to operate Window softwares, which is capable of reliable estimations of tsunami generation, propagation and evolution on coasts on easy-performable GUI environment provided by iRIC.

ELIMO ver. 4 introduced a submarine mass failure model (Watts et al. 2005) to nonlinear long wave equations to simulate tsunami induced by submarine landslide, which allows simulataneous evaluation of tsunamis caused by interplate earthquake and landslide.

Users should carefully confirm the following specifications of ELIMO and understand the model assumptions and limits of the applications. Any applications beyond the model conditions and computational accuracies used in ELIMO are not supported. It should be noted that iRIC-ELIMO cannot be held responsible for any disadvantages, loss, cost which may be incurred by ELIMO. Confirm and agree Terms of Conditions before using ELIMO.

ELIMO Development Team
Yasunori Watanabe, Hokkaido University
June, 2023

ELIMO 4.0 Specification (June 2023)

1. Governing equation; nonlinear long wave equation
2. Coordinate system; Spherical global coordinate
3. Computational method; Euler-Lagrangian finite difference method with third order accuracy (CIP metod + Predictor-Corrector method)
4. Bathymetry; General Bathymetric Chart of the Oceans (GEBCO) altitude data
5. Shore boundary condition; Impermeable condition at shore (no inundation on land area)
6. Open boundary condition; Radiation condition + Sponge zone (additional energy dissipation)
7. Fault model; Elastic rectangular fault model (Okada 1985), Tsunami generation model including horizontal fault displacements (Tanioka ad Satake 1996).
8. Submarine mass failure model (Watts et al 2005)

Contents

1 What is ELIMO? 1
- 1.1 Governing equation . . . 2
- 1.2 Computational methods and boundary conditions . . . 4
  - 1.2.1 Impermeable condition at a shore . . . 4
  - 1.2.2 Open boundary condition . . . 5
  - 1.2.3 Initial Conditions . . . 7
  - 1.2.4 Submarine landside . . . 11

2 Tutorial 13
- 2.1 Acquisition of bathymetry data . . . 13
- 2.2 Operations on iRIC . . . 16
  - 2.2.1 Generation of computing grids . . . 16
  - 2.2.2 Setting computational conditions and Executing ELIMO 18
  - 2.2.3 Run computation . . . 22
  - 2.2.4 Visualizing the results . . . 22

3 Examiples of Computations 25
- 3.1 The 2011 Tohoku earthquake tsunami . . . 25
- 3.2 Comparisons with the observed surface elevation . . . 26
- 3.3 Submarine landslide tsunami . . . 26
- 3.4 Scenario tsunami . . . 27

Update Records

1. July 2013 Release of ELIMO 1.0

2. November 2013 ELIMO 1.1; Release a format conversion software "*gebco_conv*" for GEBCO 1 minuet altitude grid data that is downloadable from British Oceanographic Data Center. The user's guide updated.

3. June 2015 ELIMO 2.0; "gebco2s2014" for 2014 format of GEBCO data has been provided. The elastic rectangular fault model by Okada (1985) and the tsunami generation model by Tanioka and Satake (1996) have been introduced. The arbitrary fault models with asperities can be used for the ELIMO computation by using a file input function for the fault parameters.

4. 2019; Allowing direct input of NetCDF GEBCO data (without preprocessing).

5. June 2023; Introducing a model for submarine landside tsunami.

Chapter 1

What is ELIMO?

A tsunami computation is a fundamental way to provide tsunami heights and arrival times along coasts for past and future earthquakes, which has been used for designing disaster prevention plans. The computations have been generally performed at high performance computers owned by Universities and research institutes, and commonly used by researchers and engineers who have scientific knowledge and experience of the numerical computation. There may be no computational tool that is accessible to the public. While the disaster prevention and evacuation plans for tsunami inundation are required to develop by local governments, they have no way to estimate the tsunami properties by their own human and computational resources. Under these background, we have tried to develop technologies for producing a compact and reliable software to compute tsunami for arbitrary earthquake, which is executable on home PC. We hope this tsunami software named ELIMO will be utilized for estimating the tsunami onsets in order to achieve disaster reduction and efficient evacuation.

iRIC is a computational platform to support computations of river flows and floods with the pre-processing functions of computational griding and the post-processing of visualizing and plotting the results on GUI environment. The tsunami solver ELIMO (Easy-performable Long-wave Inundation MOdel) is designed to perform fundamental tsunami computations on the iRIC environment.

This users guide for ELIMO is composed of three chapters. In Chapter 1, governing equations to be solved, boundary conditions, assumptions and numerical methods used in ELIMO are explained. While researchers and engineers who have scientific knowledge should confirm these technical interpretations, general users may skip this chapter. In Chapter 2, the pro-

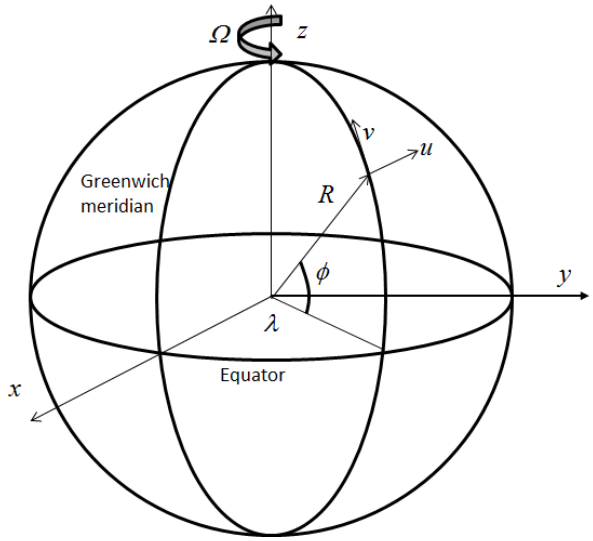

Figure 1.1: Spherical global coordinate system.

cedure to acquire bathymetry data, to compute tsunami and visualize the results is explained. Chapter 3 introduces examples of the tsunami computations, including the 2011 Tohoku earthquake tsunami.

1.1 Governing equation

The depth-averaged long wave equation is used as governing equation in ELIMO (Fig. 1.1).

$$\frac{\partial u}{\partial t}+\frac{u}{R\cos\phi}\frac{\partial u}{\partial \lambda}+\frac{v}{R}\frac{\partial u}{\partial \phi}=-\frac{1}{\rho R\cos\phi}\frac{\partial p_a}{\partial \lambda}-\frac{g}{R\cos\phi}\frac{\partial \zeta}{\partial \lambda}+\frac{\tau_\lambda^s-\tau_\lambda^b}{\rho\left(h+\zeta\right)}$$
$$+\nu_h\left(\frac{1}{R^2\cos^2\phi}\frac{\partial^2 u}{\partial \lambda^2}+\frac{1}{R^2\cos\phi}\frac{\partial}{\partial \phi}\left(\cos\phi\frac{\partial u}{\partial \phi}\right)\right)$$
$$+\left(2\Omega+\frac{u}{R\cos\phi}\right)v\sin\phi \tag{1.1}$$

$$\frac{\partial v}{\partial t}+\frac{u}{R\cos\phi}\frac{\partial v}{\partial \lambda}+\frac{v}{R}\frac{\partial v}{\partial \phi}=-\frac{1}{\rho R\cos\phi}\frac{\partial p_a}{\partial \phi}-\frac{g}{R\cos\phi}\frac{\partial \zeta}{\partial \phi}+\frac{\tau_\phi^s-\tau_\phi^b}{\rho\left(h+\zeta\right)}$$
$$+\nu_h\left(\frac{1}{R^2\cos^2\phi}\frac{\partial^2 v}{\partial \lambda^2}+\frac{1}{R^2\cos\phi}\frac{\partial}{\partial \phi}\left(\cos\phi\frac{\partial v}{\partial \phi}\right)\right)$$
$$+\left(2\Omega+\frac{u}{R\cos\phi}\right)u\sin\phi \tag{1.2}$$

where the depth-averaged mean velocities $u=\frac{1}{h+\zeta}\int_{-h}^{\zeta}u'dz$, $v=\frac{1}{h+\zeta}\int_{-h}^{\zeta}v'dz$ (local velocities u', v'), R is the distance from the center of the earth, Ω is the earth's rate of rotation, λ longitude, ϕ latitude, p_a atmospheric pressure, ζ surface elevation, ν_h coefficient of horizontal momentum exchange. Mass conservation for the depth-averaged equation system is written by

$$\frac{\partial \zeta}{\partial t}+\frac{1}{R\cos\phi}\frac{\partial}{\partial \lambda}u\left(h+\zeta\right)+\frac{1}{R\cos\phi}\frac{\partial}{\partial \phi}v\cos\phi\left(h+\zeta\right)=0 \tag{1.3}$$

Imposing zero gage pressure at the surface and ignoring surface shear, the above equations are rewritten with an additional dissipation term A_d in a sponge zone (explained in the following section) by

$$\frac{Du}{Dt}=-\frac{g}{R\cos\phi}\frac{\partial \zeta}{\partial \lambda}-\frac{\tau_\lambda^b}{\rho\left(h+\zeta\right)}+A_d u$$
$$+\nu_h^*\left(\frac{1}{R^2\cos^2\phi}\frac{\partial^2 u}{\partial \lambda^2}+\frac{1}{R^2\cos\phi}\frac{\partial}{\partial \phi}\left(\cos\phi\frac{\partial u}{\partial \phi}\right)\right)$$
$$+\left(2\Omega+\frac{u}{R\cos\phi}\right)v\sin\phi \tag{1.4}$$

$$\frac{Dv}{Dt}=-\frac{g}{R\cos\phi}\frac{\partial \zeta}{\partial \phi}-\frac{\tau_\phi^b}{\rho\left(h+\zeta\right)}+A_d v$$
$$+\nu_h^*\left(\frac{1}{R^2\cos^2\phi}\frac{\partial^2 v}{\partial \lambda^2}+\frac{1}{R^2\cos\phi}\frac{\partial}{\partial \phi}\left(\cos\phi\frac{\partial v}{\partial \phi}\right)\right)$$
$$+\left(2\Omega+\frac{u}{R\cos\phi}\right)u\sin\phi \tag{1.5}$$

$$\frac{D\zeta}{Dt}=-\frac{1}{R\cos\phi}\left(\frac{\partial uh}{\partial \lambda}+\zeta\frac{\partial u}{\partial \lambda}\right)-\frac{1}{R}\left(\frac{\partial vh}{\partial \phi}+\zeta\frac{\partial v}{\partial \phi}\right)+\frac{\tan\phi}{R}v\left(h+\zeta\right) \tag{1.6}$$

where $\frac{D}{Dt}=\frac{\partial}{\partial t}+\frac{u}{R\cos\phi}\frac{\partial}{\partial \lambda}+\frac{v}{R}\frac{\partial}{\partial \phi}$, modified bottom shear $\tau_\lambda^b=C_d|u|u$ and $\tau_\phi^b=C_d|v|v$. While many values for the drag coefficient C_d have been proposed for specific flows, $C_d=5\times10^{-3}$ is used in ELIMO.

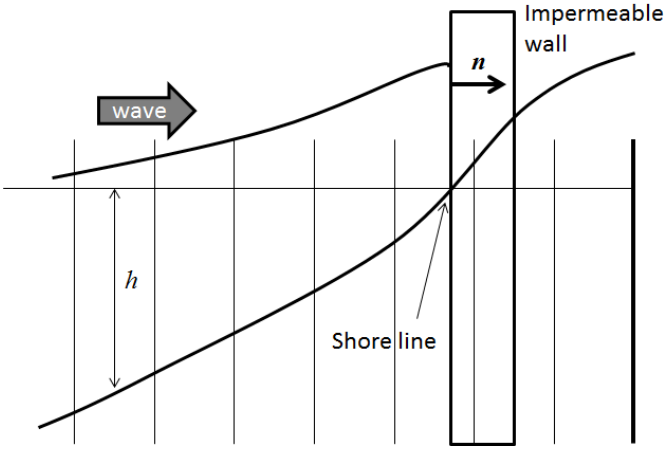

Figure 1.2: Impermeable condition at a shore

1.2 Computational methods and boundary conditions

The third order accurate, finite difference computations are performed for the nonlinear equation system Eq. (1.4)-Eq. (1.6) in the same manner as Watanabe et al. (2012); Constrained Interpolation Profile (CIP) method for the advection equation in a two-step fractional step framework, predictor-corrector method for the Eulerian terms. We don't explain the details of these numerical methods in this users guide, which can be found in the specialized literature (Goto, Okayasu and Watanabe, 2013).

1.2.1 Impermeable condition at a shore

The current version of ELIMO simply uses an impermeable condition the shore; that is, virtual vertical walls are arranged along the shore (Fig. 1.2).

The impermeable condition at a shore is expressed by

$$\frac{\partial \eta}{\partial n} = 0 \tag{1.7}$$

$$\boldsymbol{u} \cdot \boldsymbol{n} = 0 \tag{1.8}$$

where $\boldsymbol{n}$ is the normal unit vector (see Fig. 1.2).

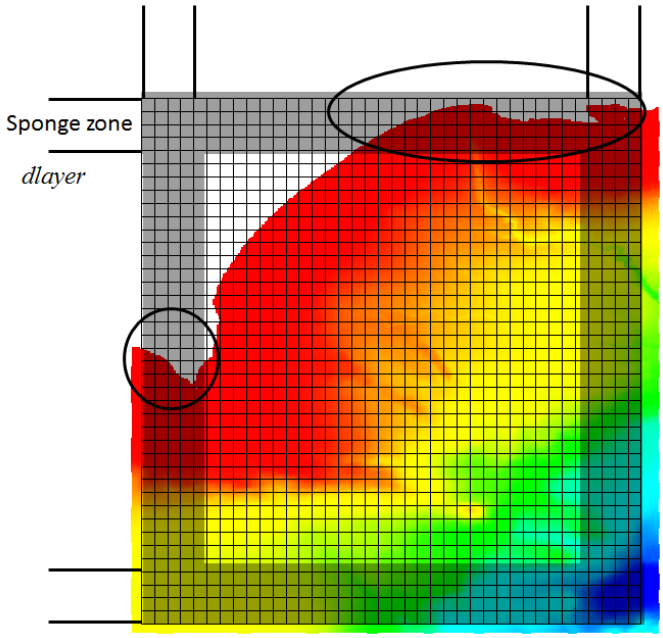

Figure 1.3: Computational domain and region to place the sponge zone (Tokachi area, Hokkaido, Japan).

1.2.2 Open boundary condition

When a finite computational domain is given in ocean area, an open boundary condition imposed at the edges of the domain is important to transmit incident waves across the boundary without any reflection. A flawed condition may induce unrealistic reflected waves at the boundaries to form multiple reflection system within the domain, which results in unacceptable computations. While a very large domain has been commonly used in the conventional tsunami computation to avoid the difficulties, e.g. a whole area of Pacific Ocean, ELIMO employs a compact domain to reduce computational loads. Therefore, appropriate open boundaries need to be given to achieve an available computation in ELIMO. While any boundary condition to achieve perfect transmission of incident waves has yet been developed, Sommerfeld's radiation condition has been commonly used (Orlanski, 1976);

$$\frac{\partial \varphi}{\partial t} + c\frac{\partial \varphi}{\partial n} = 0 \tag{1.9}$$

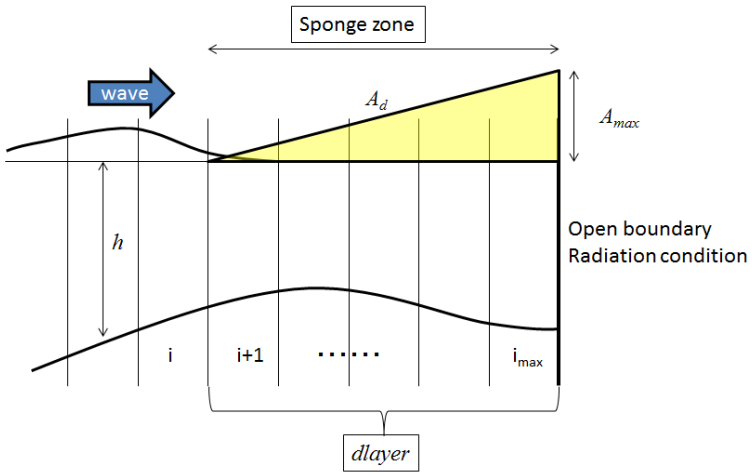

Figure 1.4: Amplification rate for the dissipation term in the sponge zone.

where the arbitrary quantity φ, and the celerity c approximated by the finite difference at the previous time step;

$$c = -\frac{\delta\varphi}{\delta t} / \frac{\delta\varphi}{\delta n} \tag{1.10}$$

δ is the finite difference operator which is constrained by the conditions;

$$c = \begin{cases} 0 & (c < 0) \\ c & (0 \le c \le \Delta x/\Delta t) \\ \Delta x/\Delta t & (c > \Delta x/\Delta t) \end{cases} \tag{1.11}$$

Significant reflection may appear under this radiation condition in the case that the celerity and incident angle spatially change near the boundary. In order to attenuate the incident waves near the boundary and to minimize the wave reflection, a so-called sponge zone is arranged at an inner area adjacent to the boundary (see Fig. 1.3).

According to Cruz et al. (1993), the dissipation coefficient A_d is given by

$$\begin{aligned} A_d &= A_{max}\sqrt{\tfrac{g}{h}}(N+1)\left(\tfrac{i-i_{max}+dlayer}{dlayer}\right)^N \quad \text{if} \quad i \ge i_{max} - dlayer \\ A_d &= 1 \qquad\qquad\qquad\qquad\qquad\qquad\qquad\qquad\qquad\qquad\quad \text{else} \end{aligned} \tag{1.12}$$

where N is the oder of the distribution function. $N = 1$ is used in ELIMO. As shown in Fig. 1.4, A_d linearly increased in the sponge zone enhances

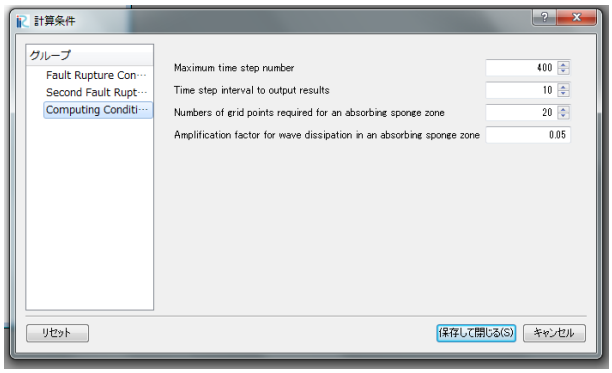

Figure 1.5: Input window for computing conditions.

dissipation for Eq. (1.4) and Eq. (1.5). As additional reflected waves may be produced within the sponge zone with too high gradients of A_d, suitable (low) A_d should be provided in the computation. While a wider sponge zone provides more dissipation, available computing area becomes smaller; that is, there is tradeoff between computational cost and performance of the boundary condition. User should carefully choose suitable number of the computing cells comprising the sponge zone ($dlayer$) and the maximum dissipation rate (A_{max}) in the window for computational conditions (see Fig. 1.5). It should be noted that tsunami is wrongly computed in coastal area containing the sponge zone as the computation is available except the sponge zone (see circles in Fig. 1.3). In this case, you should change the locations of the boundaries and use larger domain.

1.2.3 Initial Conditions

Fig. 1.6 shows the distribution of the vertical displacement of sea floor due to the 2011 Tohoku earthquake tsunami, which provided by Japan Meteorological Agency. The vertical displacement of faults directly contribute to sea level rise while the horizontal displacement also results in sea level variations over uneven sea floors.

In general, deformation of the elastic rectangular fault is determined by the fault parameters; Rupture length (L), Rupture width (W), Slip length (U), Rake angle (θ), Strike angle (ϕ), Dip angle (δ), Fault depth (d), Latitude and Longitude of Fault Top（see Fig. 1.7 and Fig. 1.8）. ELIMO uses the elastic fault model for the rectangular dip-slip deformation source, which is derived by Okada (1985). This model provides the three-dimensional

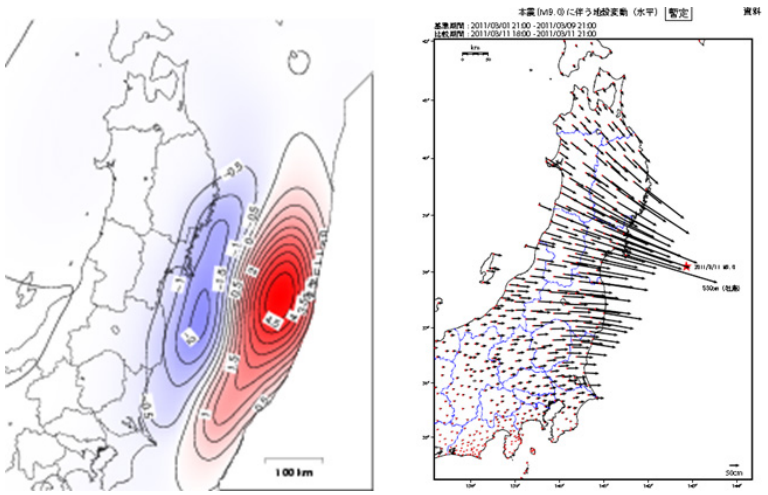

Figure 1.6: Displacement of sea floor due to the 2011 Tohoku earthquake tsunami; vertical displacement (left) and horizontal one (right) (web page of Japan Meteorological Agency).

displacements at arbitrary coordinate (x, y).

$$u_x = -\frac{U_2}{2\pi}\left(\frac{q}{R} - I_3 \sin\delta\cos\delta\right) \tag{1.13}$$

$$u_y = -\frac{U_2}{2\pi}\left(\frac{\tilde{y}q}{R\,(R+\xi)} + \cos\delta \arctan\frac{\xi\eta}{qR} - I_1 \sin\delta\cos\delta\right) \tag{1.14}$$

$$u_z = -\frac{U_2}{2\pi}\left(\frac{\tilde{d}q}{R\,(R+\xi)} + \sin\delta \arctan\frac{\xi\eta}{qR} - I_5 \sin\delta\cos\delta\right) \tag{1.15}$$

$$\tag{1.16}$$

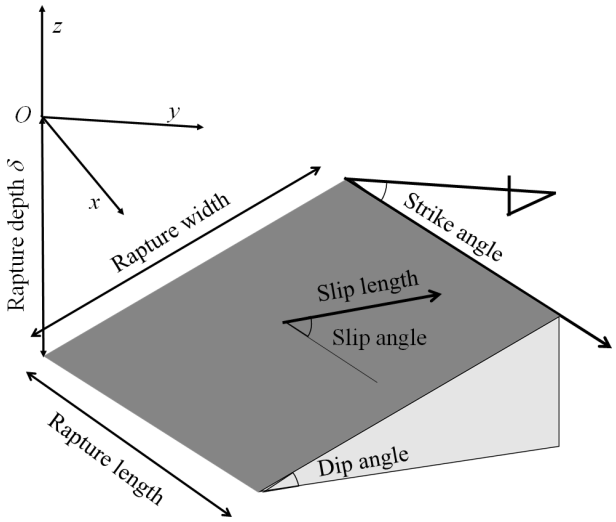

Figure 1.7: Fault parameters; slip length, slip angle, strike and dip angle.

where

$$I_1 = -\frac{\mu}{\lambda+\mu}\frac{\xi}{\left(R+\tilde{d}\cos\delta\right)} - I_5\tan\delta \tag{1.17}$$

$$I_2 = -\frac{\mu}{\lambda+\mu}\log\left(R+\eta\right) - I_3 \tag{1.18}$$

$$I_3 = \frac{\mu}{\lambda+\mu}\left(\frac{\tilde{y}}{\cos\delta\left(R+\tilde{d}\right)} - \log\left(R+\eta\right)\right) - I_4\tan\delta \tag{1.19}$$

$$I_4 = \frac{\mu}{\lambda+\mu}\frac{1}{\cos\delta}\left(\log\left(R+\tilde{d}\right) - \sin\delta\log\left(R+\eta\right)\right) \tag{1.20}$$

$$I_5 = \frac{\mu}{\lambda+\mu}\frac{2}{\cos\delta}\arctan\frac{\eta\left(X+q\cos\delta\right)+X\left(R+X\right)\sin\delta}{\xi\left(R+X\right)\cos\delta} \tag{1.21}$$

$$\tag{1.22}$$

and $p = y\cos\delta + d\sin\delta$, $q = y\sin\delta - d\cos\delta$, $\tilde{y} = \eta\cos\delta + q\sin\delta$, $\tilde{d} = \eta\sin\delta - q\cos\delta$, $R^2 = \xi^2+\eta^2+q^2 = \xi^2+\tilde{y}^2+\tilde{d}^2$, $X^2 = \xi^2+q^2$, U_2 is the dip-slip displacement source. These displacements are evaluated by using the following relation;

$$f(\xi,\eta) = f(x,p) - f(x,p-W) - f(x-L,p) + f(x-L,p-W). \tag{1.23}$$

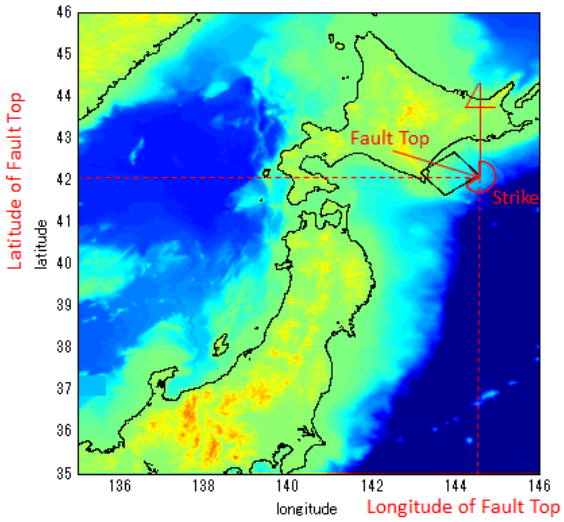

Figure 1.8: Fault parameters; longitude and latitude of the fault top, and strike (in the case of the 2003 Tokachi-off earthquake)

Fig. 1.9 shows the vertical and horizontal displacements of the sea floor for the fault parameters for the 2003 Tokachi off earthquake, estimated by the Okada's model. Any sea floor displacements for arbitrary fault parameters can be determined by this model.

Tanioka and Satake (1995) proposed the tsunami generation model to use as an initial sea level condition (ζ), based on bulk water displacement due to horizontal sea floor displacement as well as direct water displacement by vertical sea floor displacement;

$$\zeta = u_z + u_x \frac{\partial h}{\partial x} + u_y \frac{\partial h}{\partial y} \tag{1.24}$$

ELIMO determines the initial sea level by the Tanioka-Satake model using the Okada's solutions for the input fault parameters. Users can choose two options to input the parameters, 'manual input' and 'file input', on ELIMO, and in particular, the latter option is useful for setting up spatially-non-uniform displacements described by local deformation of multiple fault segments, which will be explained in §2.2.2.

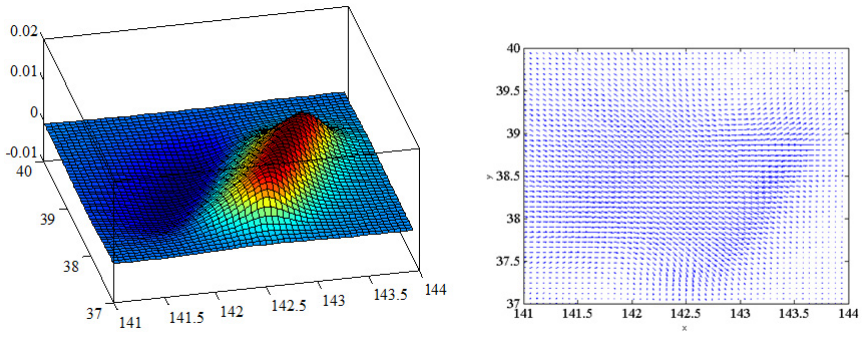

Figure 1.9: Vertical (left) and horizontal (right) displacements for the 2003 Tokachi off earthquake.

1.2.4 Submarine landside

Watts et al. (2005) developed a Submarine Mass Failure (SMF) model, defining initial sea-level displacement when submarine landslide occurs. According to their model, characteristic tsunami amplitude owing to the landslide is given by

$$\eta_0 \approx 1.74 \times 10^{-5} b \left(1 - 0.750 \sin\theta\right) \left(\frac{b \sin\theta}{d}\right)^{1.75} \tag{1.25}$$

where b is the length of SMF, d is the water depth at the maximum thickness of initial SMF, θ is the bed slope. The initial surface form at arbitrary location (x, y) was approximated by a double Gaussian distribution in x-direction and a soliton-like wave form in y-direction with respect to the initial location of SMF (x_0, y_0);

$$\eta(x,y) \approx -\frac{\eta_0}{\eta_{min}} \mathrm{sech}^2 \left(\kappa \frac{y - y_0}{w + \lambda_0}\right) \left(\mathrm{e}^{-\left(\frac{x-x_0}{\lambda_0}\right)^2} - \kappa' \mathrm{e}^{-\left(\frac{x-\Delta x-x_0}{\lambda_0}\right)^2}\right) \tag{1.26}$$

where $\kappa \approx 3$, w is the width of SMF, λ_0 is the characteristic wavelength, κ' and Δx are parameters controling double Gaussian surface forms. η_{min} indicates the minimum value of the function on the right-hand side of Eq. (1.26) (excluding the amplitude). According to characteristic tsunami scalings, characteristic time $t_0 = u_t/a_0$, terminal speed $u_t = \sqrt{gb}\sqrt{\pi\left(\gamma - 1\right)\sin\theta/2C_d}$, initial acceleration $a_0 = g \sin\theta \left(\gamma - 1\right) / \left(\gamma + C_m\right)$, characteristic wavelength $\lambda_0 = t_0\sqrt{gd}$. Here, γ is the specific gravity, C_d is the drag coefficient, C_m

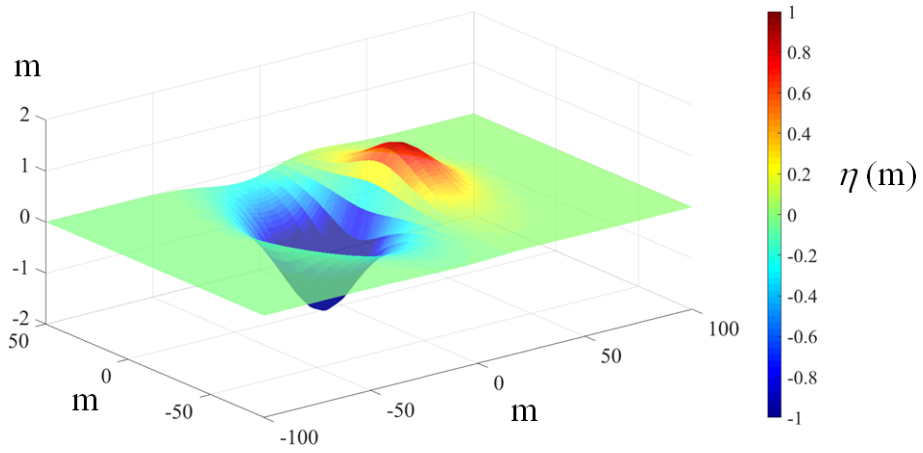

Figure 1.10: An example of initial surface elevation estimated by Eq. (1.26); b=50m, d=5m, κ=3, Δx=10m, w=25m, λ_0=25m, κ'=0.8

is the added mass coefficient. The submarine landside tsunami can be simulated through computations of nonlinear long wave equations under the initial surface elevation defined by Eq. (1.26) with these specific parameters.

Chapter 2

Tutorial

This chapter describes a whole procedure to simulate and analyze tsunami; acquisition of bathemetry data, import of the bathemetry file, generation of computing grids, setup of initial conditions (fault rapture parameters, computing conditions), execution of ELIMO, visualizing and analyzing computed results.

2.1 Acquisition of bathymetry data

ELIMO 4.0 uses netCDF bathmetry data provided by General Bathymetric Chart of the Oceans (GEBCO). As the GEBCO covers the whole area of the earth, we can simulate tsunamis occurring anywhere in oceans. The data can be downloaded in the following procedure;

1. In the web site of the General Bathymetric Chart of the Oceans (GEBCO) `https://www.gebco.net/`, click 'Download GEBCO's global grid' (bule rectangure bottom on the top left in Fig. 2.1) .
2. Click the world map (Fig. 2.2) bellow 'Download data for user-defined areas'.
3. Fill in latitude and longitude of boundaries of the rectangular area to download in 'ENTER BOUNDARY' on the left side of the world map, or specify the rectangular area by dragging mouse with holding 'Ctrl'.
4. In `SELECT FORMATS' (left input space), click a check box for 2D netCDF and Grid (top left check box).

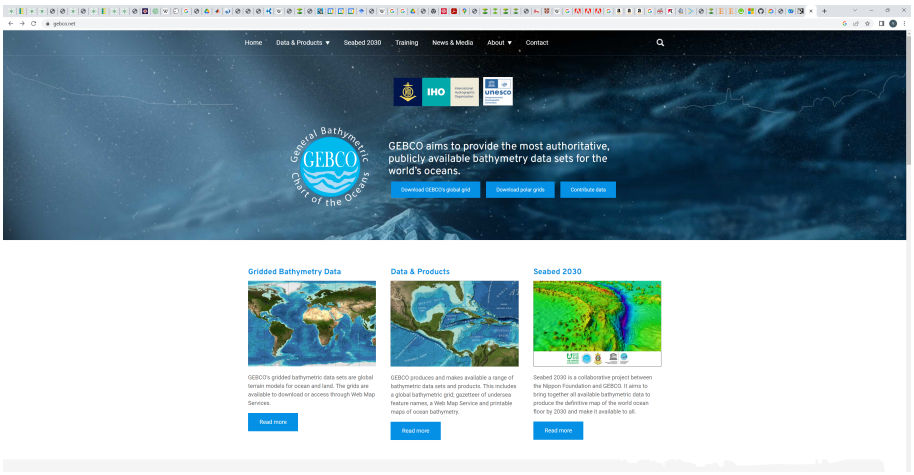

Figure 2.1: Web site of GEBCO

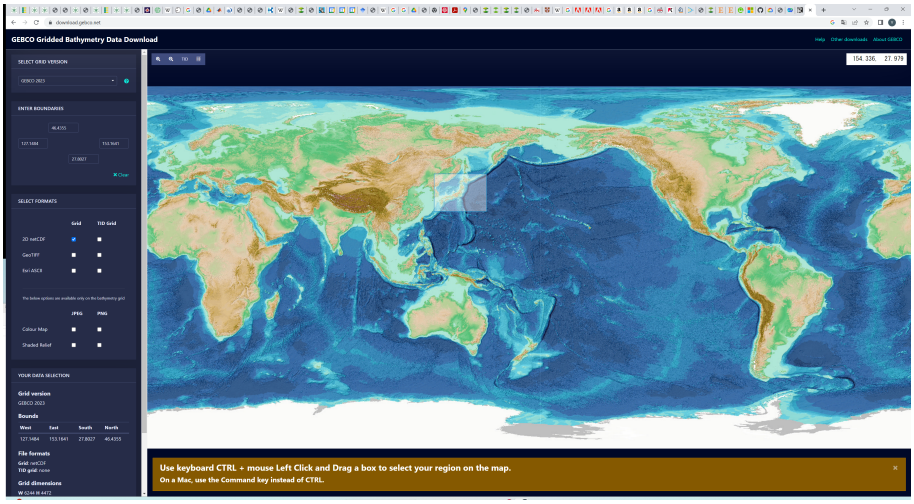

Figure 2.2: Specify a region to download

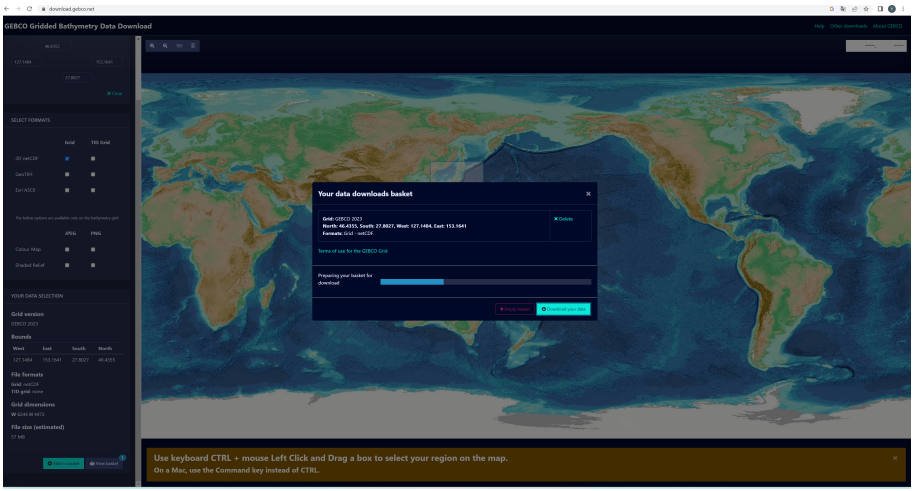

Figure 2.3: Download the bathymetry data

5. Click ‘Add to basket’ (bottom button in left input space). Then, click the neighboring button ‘View basket’.

6. Click a right bottom button ‘Download your data’ on a popup window (Fig. 2.3).

7. Move the downloaded data to a folder used for your computation.

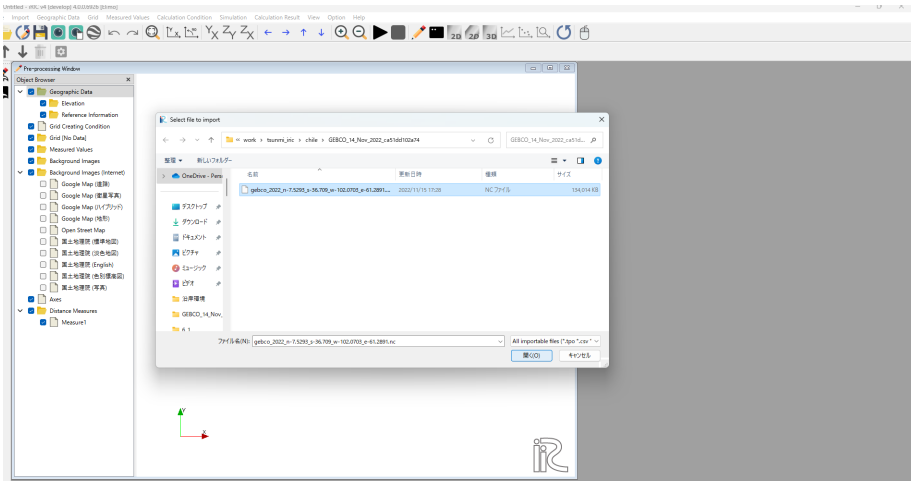

Figure 2.4: Importing bathymetry data file

2.2 Operations on iRIC

The procedures to compute tsunami and visualize the results are explained below.

2.2.1 Generation of computing grids

1. Run iRIC.
2. Choose ‘File’ → ‘New Project’. Choose ’ELIMO’ in the window ‘Select Solver’.
3. Confirm ‘Pre-processing window’ is generated. Choose ‘Import’→‘Geographic Data’→‘Elevation’.
4. Choose your downloaded GEBCO file (Fig. 2.4).
5. Click ‘OK’ on a popup window telling ‘To import the geographic data, specify coordinate system for the project first’.
6. Type ‘wgs’ in a search work box on a popup window of ‘Select Coordinate System’. You will then find ‘EPSG:4326:WGS 84’ in the list of coordinates. Click this coordinate (see Fig. 2.5).

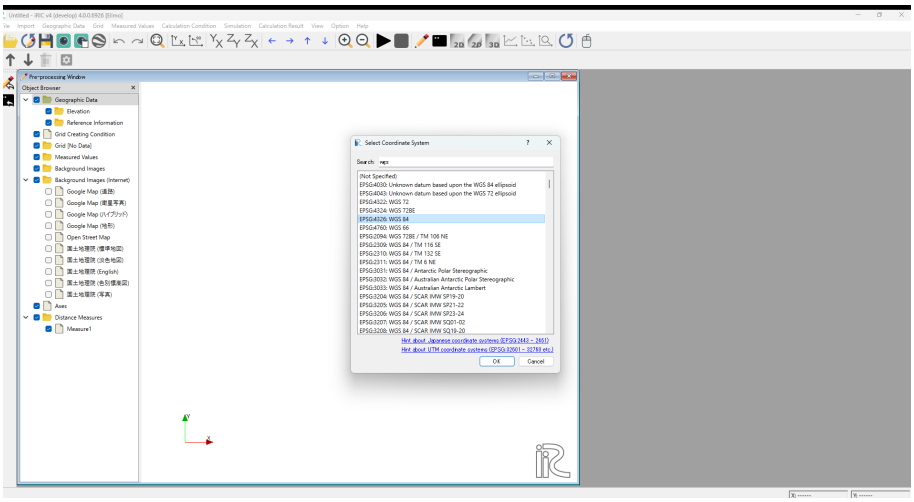

Figure 2.5: Setting coordinates

7. Confirm the imported bathymetry is identical with the area you want to compute.

8. Menu 'Grid'→'Select Algorithm to Create Grid'. Choose 'Create grid by dividing rectangular region (Longitude-Latitude)' in the window 'Select Grid Creating Algorithm'.

9. Define the computational domain by a mouse within the area of the imported bathymetry (Fig. 2.6). Note that the computational domain has to be smaller than the imported bathymetry area, and should be inside any bathymetry data boundaries.

10. Choose 'Grid'→'Create Grid'. Define a grid width 'd' to be the resolution that you want to compute at. Since the global coordinate system is used in ELIMO, x-axis represents longitude and y-axis is latitude (i. e. d=0.1 degrees may indicate the grid width over 6 km). As computational costs increase with the resolution, User should choose the optimal grid width in terms of resolution and cost. The grid width d to be in a range of 0.01 and 0.02 degrees (36 – 72 second) is recommended. As GEBCO has the resolution of 15 sec, user can compute at higher resolution, while there may be interference between the grid locations of the bathmetry data and computing grids (especially near shore lines). If you find strange computed results (such as strange

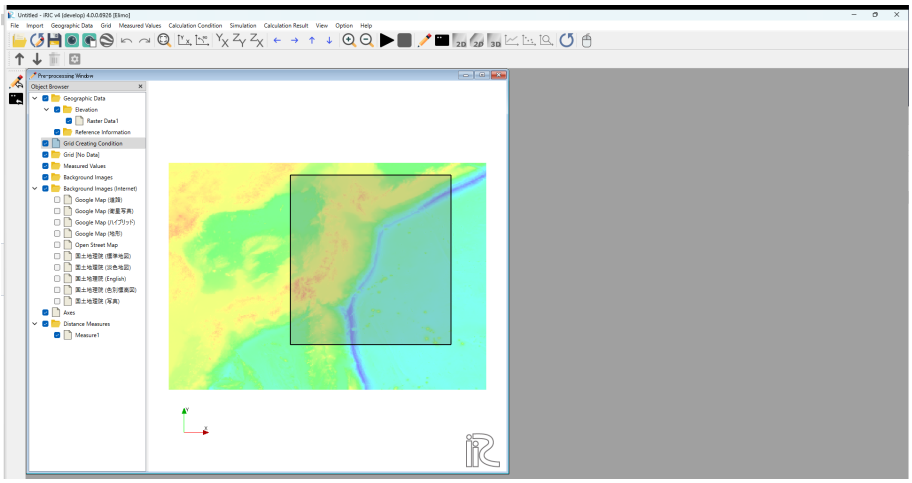

Figure 2.6: Generating a computing domain

waves generated before arriving tsunami), reconsider the grid width d.

11. Click 'OK' on the popup window.

2.2.2 Setting computational conditions and Executing ELIMO

Menu 'Calculation Condition' → 'Setting', then appearing a window 'Calculation Condition'. Each group in the left box is explained bellow (Fig. 2.7).

File Input of Falut Rapture Conditions

If you answer for "Which manner to input fault conditions?" is "Manual Input", you should manually input fault parameters for interplate earthquake tsunami. If you select "File Input", click the button on the right of "File Name of Fault Conditions" and select your parameter file on the dialog box.

Fault Rapture Conditions (Manual)

This method is useful to manually input the parameters for one or two rectangular faults on the input window of ELIMO. For instance, the two faults models for the 2011 Tohoku earthquake tsunami have been proposed by the Geospatial Information Authority of Japan (Table 3.1). To provide multiple fault displacements following this model, fill in parameters on the

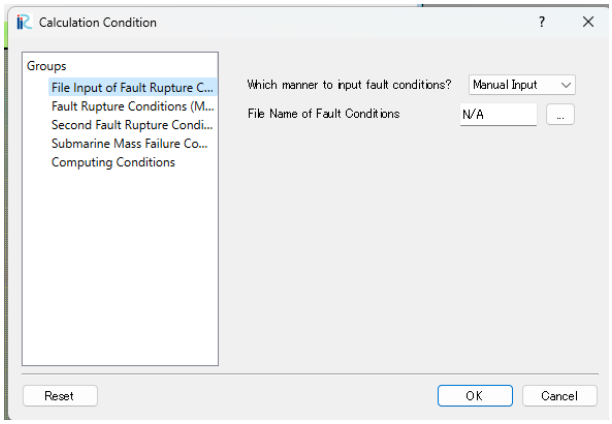

Figure 2.7: Window of Calculation Condition

Table 2.1: Rectangle fault model for the 2011 Tohoku earthquake with following parameters provided by the Geospatial Information Authority of Japan

	latitude (^{o})	latitude (^{o})	length (km)	width (km)	slip length (m)	strike (^{o})	dip (^{o})	rake (^{o})	Fault depth (km)
Fault 1	39.00	143.49	199	85	27.7	202	18	97	10.0
Fault 2	37.21	142.51	176	82	5.9	201	15	81	10.1

first fault in 'First Fault Rupture Conditions' and parameters on the second one in 'Second Fault Rupture Conditions'. Default parameters for the 2003 Tokachi-off earthquake tsunami have been provided. For any fault model with a single rapture, all parameters for 'Second Fault Rapture Conditions' should be given to be zero. It should be noted that 'Fault depth' is defined by depth of the fault bottom d in ELMO (see Fig. 1.7) while depth at the fault top d_{top} may be used in some fault models for scenario tsunami. d can be estimated with d_{top} by

$$d = d_{top} + W \tan\delta \sin\theta \tag{2.1}$$

where δ is the dip angle, W is the rapture width and θ is the rake angle.

File input of the fault parameters

Fault models for past and scenario tsunami, commonly provided, are composed by many fault segments to describe asperity and local orientation of

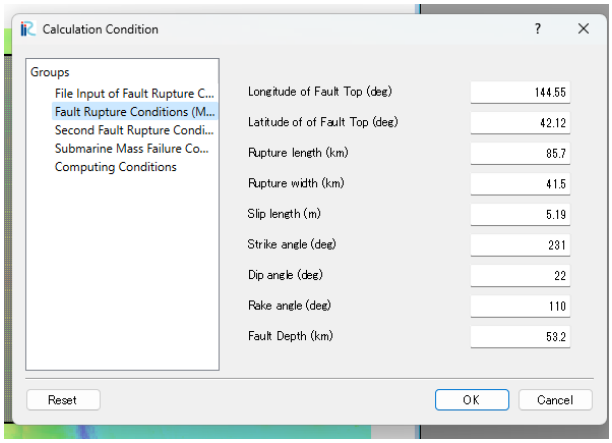

Figure 2.8: Input window for fault parameters

the raptures (Fig. 2.9). In ELIMO, arbitrary fault parameters for multiple segments can be given by a batch file input. For instance, if the parameters for 12 segments described in Fig. 2.9 are provided by Table 2.2 (These parameters will be explained again in §4), as shown in Fig. 2.10, the parameters for each segment are described on each line in order of latitude, longitude, rapture length, rapture width, slip-length, strike, dip, rake and fault depth with space or comma separation. It should be noted that 'Fault depth' is defined by depth of the fault bottom d in ELMO (see Fig. 1.7). If depth at the fault top d_{top} is defined in past fault models, d estimated by Eq. (2.1) needs to be provided in the file. Add lines for the parameters of all segments; in the case of Fig. 2.9, every parameters of 12 lines should be written and saved with arbitrary file name.

Submarine Mass Failure Conditions (Manual)

Parameter input for submarine landslide tsunami using SMF model is explained bellow.

For "Which tsunami to compute?", select "Plate Boundary Earthquake Tsunami Only", "Submarine Landslide Tsunami Only", or "Both". Input the following parameter (see section 1.2.4);

1. "Longitude of SMF center (deg)"
2. "Latitude of SMF center (deg)"

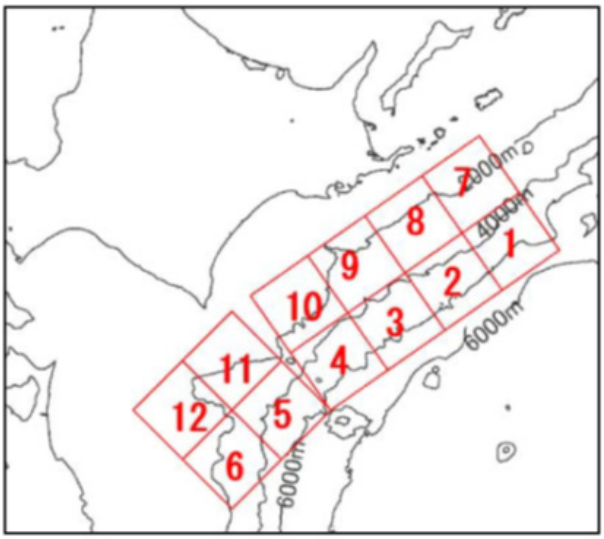

Figure 2.9: Fault segments of the scenario tsunami of Hokkaido off earthquake.

3. "Latitude of SMF center (deg)"
4. "Length of SMF along seabed slope (km)"; b
5. "Width of SMF (km)";w
6. "Characteristic wavelength; lambda0 (km)"; λ_0
7. "Parameter Kappa'"; parameter controlling double Gaussian distribution κ' (ratio of positive and negative initial surface displacements in Fig. 1.10)
8. "Parameter Delta x (km)"; shape parameter of double Gaussian distribution Δx (km)

Here depth of initial SMF d and bed slope θ are automatically estimated from the bathymetry data. κ=3 is given as constant.

Computing Conditions

Input the maximum time step number, time-step interval for saving output files (e.g. if 3 is given, the data files are saved every 3 time steps) , number

	longitude (^{o})	latitude (^{o})	length (km)	width (km)	slip length (m)	strike (^{o})	dip (^{o})	rake (^{o})	depth (fault top) (km)
Fault 1	147.5584	42.4135	70.0	70.0	35.0	235	10	90	5.0
Fault 2	146.8476	42.0703	70.0	70.0	35.0	235	10	90	5.0
Fault 3	146.1445	41.7226	70.0	70.0	35.0	235	10	90	5.0
Fault 4	145.4488	41.3704	70.0	70.0	35.0	235	10	90	5.0
Fault 5	144.7606	41.0140	70.0	70.0	35.0	225	10	90	5.0
Fault 6	144.1726	40.5693	70.0	70.0	35.0	225	10	90	5.0
Fault 7	147.0946	42.9421	70.0	70.0	30.0	235	20	90	17.0
Fault 8	146.3802	42.5962	70.0	70.0	30.0	235	20	90	17.0
Fault 9	145.6735	42.2457	70.0	70.0	30.0	235	20	90	17.0
Fault 10	144.9746	41.8907	70.0	70.0	30.0	235	20	90	17.0
Fault 11	144.1716	41.4608	70.0	70.0	30.0	225	20	90	17.0
Fault 12	143.5836	41.0132	70.0	70.0	30.0	225	20	90	17.0

Table 2.2: Fault parameters for the segments of the scenario tsunami of Hokkaido off earthquake (corresponding to Fig. 2.9).

of grids contained in a sponge zone (*dlayer* in §1.2.2), and the maximum dissipation rate in a sponge zone (A_{max} in §1.2.2). *dlayer* and A_{max} may be adjusted if unacceptable reflection occurs at the open boundaries (depending on size and location of the computing domain).

Confirming the computing conditions

Click 'OK' on the window of 'Calculation Condition'.

2.2.3 Run computation

Menu 'Simulation' → 'Run'. Duration from the tsunami generation is displayed on a console screen.

2.2.4 Visualizing the results

How to visualize the results is explained in iRIC Users Manual; such as contours, vector plots, animation of the results. In this chapter, only particular operations required in ELIMO are explained.

1. 'Calculation Result' → 'Open new 2-D Post-Prosessing Window'
2. Click a check box of 'SElevation' in 'Elimo Grids'¿'iRIVZone'¿'Scalar' on Object Browser (Fig. 2.11).

```
147.5584 42.4135 70.0 70.0 35.0 235 10 90 17.3
146.8476 42.0703 70.0 70.0 35.0 235 10 90 17.3
146.1445 41.7226 70.0 70.0 35.0 235 10 90 17.3
145.4488 41.3704 70.0 70.0 35.0 235 10 90 17.3
144.7606 41.0140 70.0 70.0 35.0 225 10 90 17.3
144.1726 40.5693 70.0 70.0 35.0 225 10 90 17.3
147.0946 42.9421 70.0 70.0 30.0 235 20 90 42.5
146.3802 42.5962 70.0 70.0 30.0 235 20 90 42.5
145.6735 42.2457 70.0 70.0 30.0 235 20 90 42.5
144.9746 41.8907 70.0 70.0 30.0 235 20 90 42.5
144.1716 41.4608 70.0 70.0 30.0 225 20 90 42.5
143.5836 41.0132 70.0 70.0 30.0 225 20 90 42.5
```

Figure 2.10: Parameter text file for the file input.

3. Right click on 'SElevation' and select 'Property' to set up graphycs (color bar, color range and so on).

4. When you choose one on the list of 'Background Images (Internet)' on Object Browser, your result is superposed on the selected map (Fig. 2.11).

5. Sequential images of the computed results every output time step are displayed if you operate in menu 'Animation'.

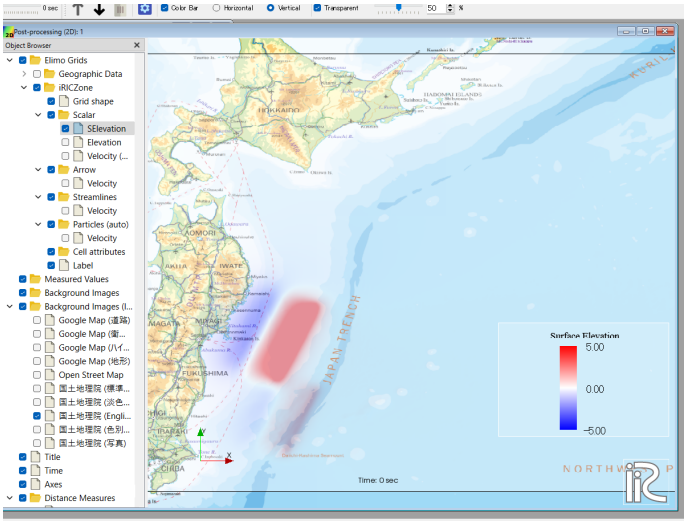

Figure 2.11: Visualized surface elevation 「SElevation」

Chapter 3

Examiples of Computations

3.1 The 2011 Tohoku earthquake tsunami

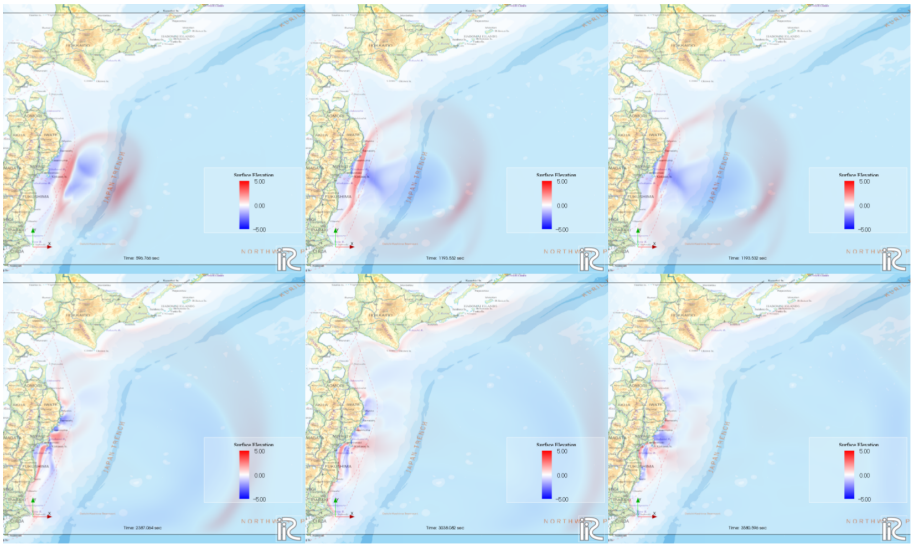

Figure 3.1: Propagation of the 2011 Tohoku tsunami (10 min interval from tsunami generation).

The Geospatial Information Authority of Japan provided the rectangle fault model for the 2011 Tohoku earthquake with following parameters. In this model, the depth of fault is defined at the top of fault. The fault depths, defined at the bottom in ELIMO, are estimated by Eq. (2.1) to be 37.4 km

	latitude (^{o})	latitude (^{o})	length (km)	width (km)	slip length (m)	strike (^{o})	dip (^{o})	rake (^{o})	Fault depth (km)
Fault 1	39.00	143.49	199	85	27.7	202	18	97	10.0
Fault 2	37.21	142.51	176	82	5.9	201	15	81	10.1

and 31.8 km. Therefore, the estimated depths, 37.4 and 31.8, need to be described on 'First and Second Rapture Condistions' instead of 10.0 and 10.1 in Table 3.1. As many fault models using the depth of fault top have been proposed, Use should confirm the definition of the parameter used in the model.

Fig. 3.1 shows the contours of the surface elevation of the tsunami until one hour after the earthquake. It is seen that the tsunami radically spreads at an early stage, arrives to Iwate prefecture at 10 – 15 minutes, Hokkaido and Kita-Kanto areas after one hour. These computed arrival of the tsunami are consistent with the observed ones.

3.2 Comparisons with the observed surface elevation

Kawai et al. (2013) reported the surface elevation of the 2011 Tohoku tsunami measured by GPS buoys installed Tohoku off. Fig. 3.2 shows the observed surface elevations presenting rapid evolution of the tsunami wave shapes.

Fig. 3.3 shows the initial stage of the computed surface elevations at the corresponding locations to the GPS stations. We find overall features of the computed tsunami evolution are consistent with the observed ones despite that the simplest rectangular fault model are used in the computation. Improvement of accuracy is expected by introducing polished fault models with asperity.

3.3 Submarine landslide tsunami

M 7.5 earthquake occurred on Sulawesi, Indnesia o the 28th of September, 2018. Tsunami has been observed around coast of Palu Bay after 30 min later the earthquake. The analyses of this tsunami conclude submarine landslides induced by the earthquake generated the tsunami (Nakata et al. 2020).

While there have been many studies on magnitude and area of landslide, as an application of SMF model, the computed tsunami based on a scenario

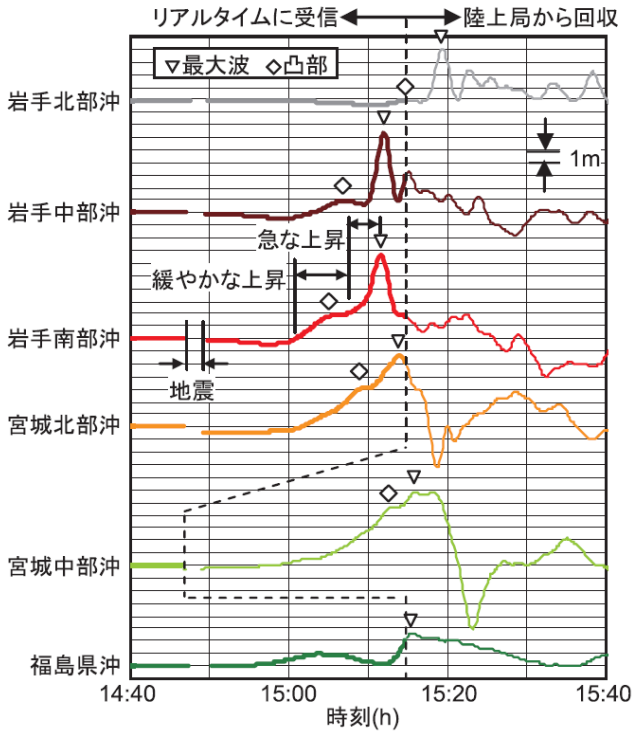

Figure 3.2: Observed surface elevations at the GPS tide stations (After Kawai et al. 2013).

that a submarine landslide occurred off Palu is shown here.

Fig. 3.4 shows evolution of the submarine landslide tsunami. While resolution of bathymetry data is not enough to compute local tsunami near the coast, overall features of the propagation with reflection in the bay can be found from the results.

3.4 Scenario tsunami

Many fault models for scenario tsunamis, expected to occur in future, have been proposed by the governments and research institutes, which provides possible tsunami heights along coasts of Japan. Most models composed of multiple fault segments can be used on ELIMO by the function of the batch file input.

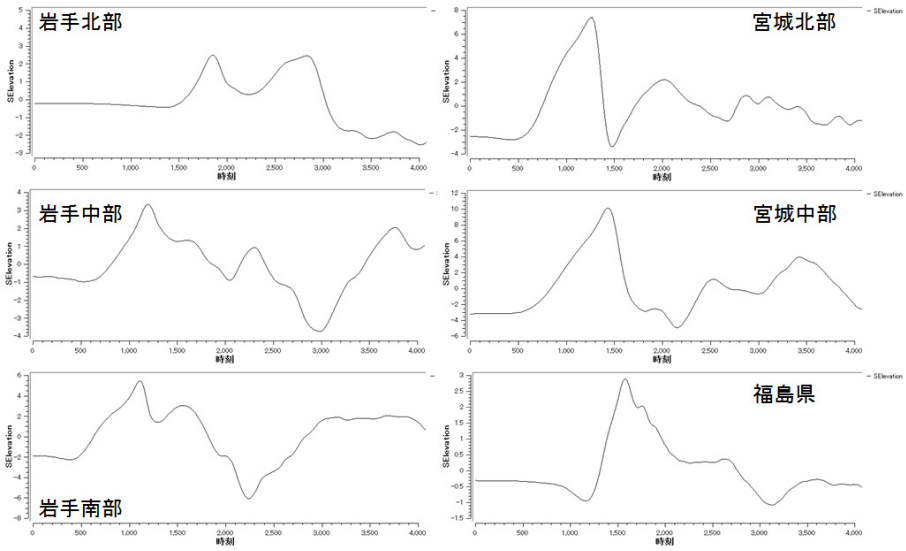

Figure 3.3: Computed surface elevations at the GPS tide stations.

The government of Hokkaido, Japan, defined the scenario tsunami that may cause the maximum inundation on Pacific coasts of Hokkaido, and provided the fault model. In this model for the extreme tsunami, 12 fault segments with the parameters in Table 3.1 are assumed to adjacently locate as shown in Fig. 3.5.

The text parameter file for Table 3.1 are shown in Fig. 3.6. The line number corresponds to the fault number. The parameters for each segment,latitude, longitude, rapture length, rapture width, slip-length, strike, dip, rake and fault depth with space or comma separation, are described on each line. As already explained, 'Fault depth' is defined by depth of the fault bottom d in ELMO (see Fig. 1.7). If depth at the fault top d_{top} is defined in past fault models, d estimated by Eq. (3.1) needs to be provided in the file.

$$d = d_{top} + W \tan\delta \sin\theta \tag{3.1}$$

where δ is the dip angle, W is the rapture width and θ is the rake angle.

For example, for Fault 1 – 6, $5+70\times\tan(10\times\pi/180)\times\sin(90\times\pi/180) \approx 17.3$, and for 7 -12, $17 + 70 \times \tan(20 \times \pi/180) \times \sin(90 \times \pi/180) \approx 42.5$ should be written in the file as 'Fault depth' instead of 5.0 and 17.0. Every parameters of 12 lines are written and saved with arbitrary file name for the batch input.

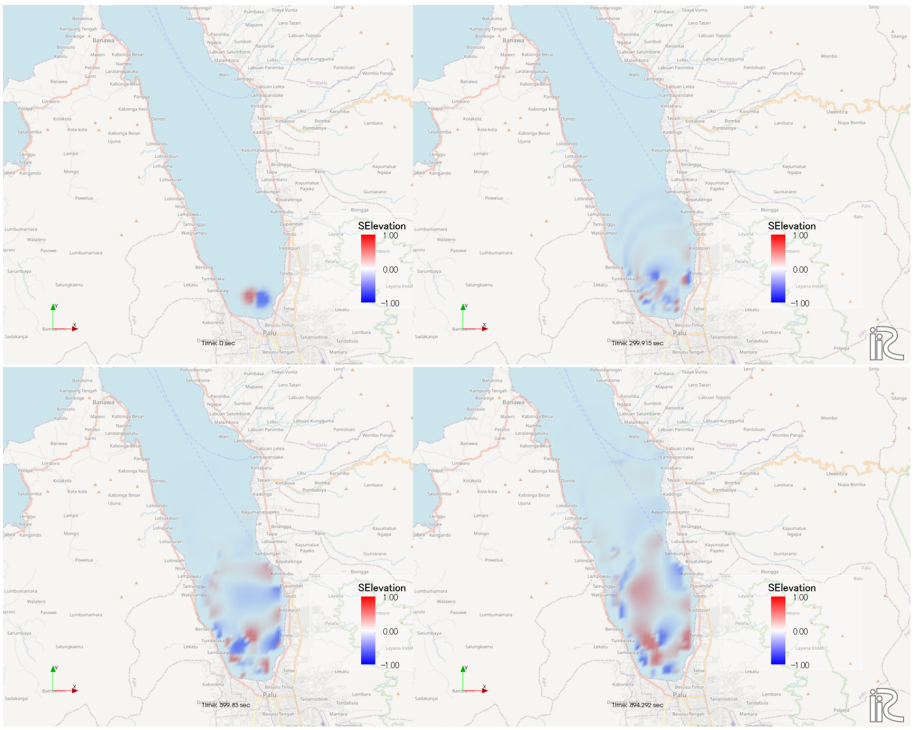

Figure 3.4: Sea level changes owing to the 2018 Palu tsunami, Sulawesi, Indonesia (5 min interval)

Fig. 3.7 shows the evolution of the Hokkaido scenario tsunami generated by the model of Table 3.1 . The tsunami, generated by the fault displacements over a wide area, radically propagates and reach to the Pacific coasts after 10 – 20 minutes. The first wave of tsunami arrives at most coasts of Hokkaido and Tohoku after 30 minutes, and formations of edge waves are confirmed after 50 minutes.

Fig. 3.8 presents the computed surface elevations (not by ELIMO) reported by the government of Hokkaido. We find the analogous features of tsunami elevations to Fig. 3.7.

I this way, ELIMO can simulate arbitrary tsunami generated by any model without any limitation of number of segments.

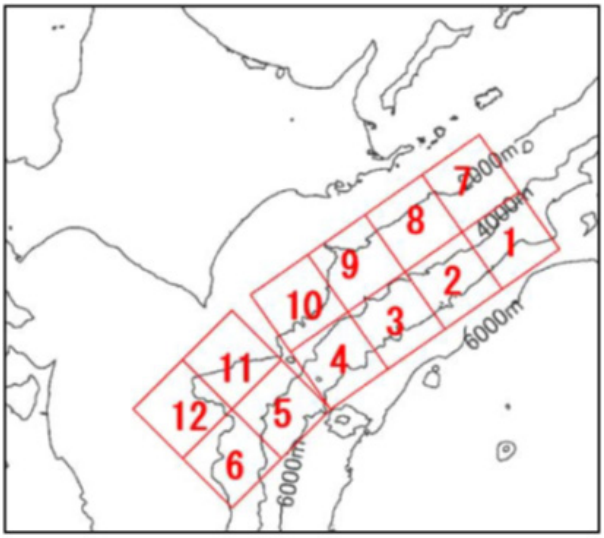

Figure 3.5: Fault segments of the scenario tsunami of Hokkaido off earthquake.

	longitude (^{o})	latitude (^{o})	length (km)	width (km)	slip length (m)	strike (^{o})	dip (^{o})	rake (^{o})	depth (fault top) (km)
Fault 1	147.5584	42.4135	70.0	70.0	35.0	235	10	90	5.0
Fault 2	146.8476	42.0703	70.0	70.0	35.0	235	10	90	5.0
Fault 3	146.1445	41.7226	70.0	70.0	35.0	235	10	90	5.0
Fault 4	145.4488	41.3704	70.0	70.0	35.0	235	10	90	5.0
Fault 5	144.7606	41.0140	70.0	70.0	35.0	225	10	90	5.0
Fault 6	144.1726	40.5693	70.0	70.0	35.0	225	10	90	5.0
Fault 7	147.0946	42.9421	70.0	70.0	30.0	235	20	90	17.0
Fault 8	146.3802	42.5962	70.0	70.0	30.0	235	20	90	17.0
Fault 9	145.6735	42.2457	70.0	70.0	30.0	235	20	90	17.0
Fault 10	144.9746	41.8907	70.0	70.0	30.0	235	20	90	17.0
Fault 11	144.1716	41.4608	70.0	70.0	30.0	225	20	90	17.0
Fault 12	143.5836	41.0132	70.0	70.0	30.0	225	20	90	17.0

Table 3.1: Fault parameters for the segments of the scenario tsunami of Hokkaido off earthquake (corresponding to Fig. 2.9).

```
147.5584 42.4135 70.0 70.0 35.0 235 10 90 17.3
146.8476 42.0703 70.0 70.0 35.0 235 10 90 17.3
146.1445 41.7226 70.0 70.0 35.0 235 10 90 17.3
145.4488 41.3704 70.0 70.0 35.0 235 10 90 17.3
144.7606 41.0140 70.0 70.0 35.0 225 10 90 17.3
144.1726 40.5693 70.0 70.0 35.0 225 10 90 17.3
147.0946 42.9421 70.0 70.0 30.0 235 20 90 42.5
146.3802 42.5962 70.0 70.0 30.0 235 20 90 42.5
145.6735 42.2457 70.0 70.0 30.0 235 20 90 42.5
144.9746 41.8907 70.0 70.0 30.0 235 20 90 42.5
144.1716 41.4608 70.0 70.0 30.0 225 20 90 42.5
143.5836 41.0132 70.0 70.0 30.0 225 20 90 42.5
```

Figure 3.6: Parameter text file for the file input.

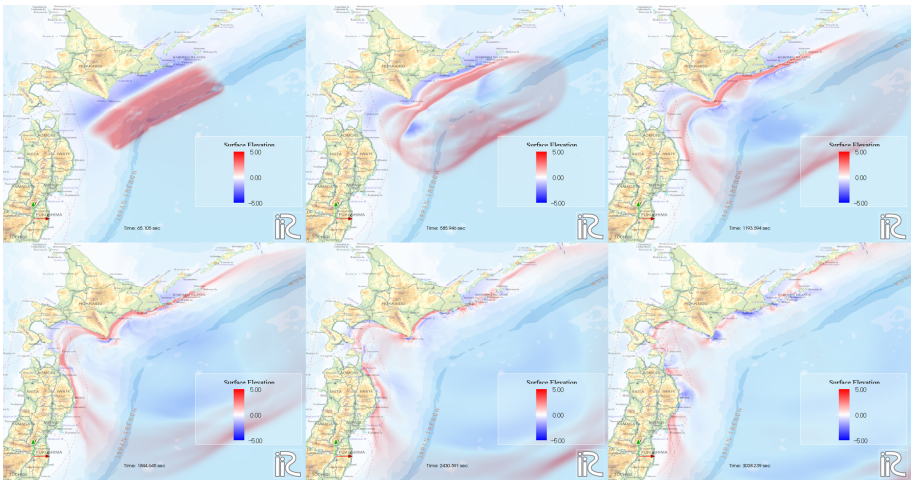

Figure 3.7: The surface elevations along Hokkaido coasts by Hokkaido scenario tsunami, computed by ELIMO (10 minutes intervals).

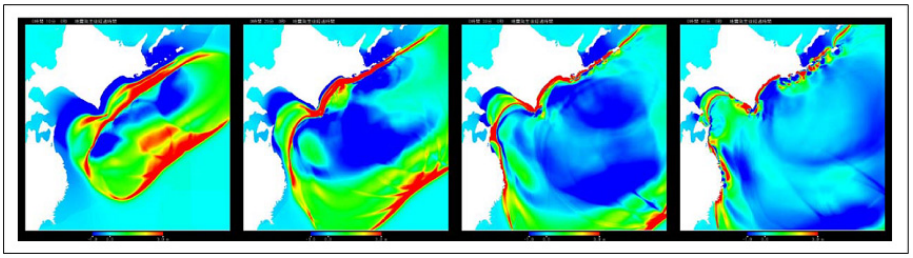

Figure 3.8: The surface elevations along Hokkaido coasts by Hokkaido scenario tsunami, reported by the local government of Hokkaido.

Conculding Remarks

Large earthquakes exceeding M8 are expected in near future, such as Tokai, Nankai trough and Nemuro-off earthquakes. Multiple approaches for reducing tsunami disaster and minimizing damage expected for such earthquake should be considered in a rush. We hope ELIMO that enables general users to perform the tsunami computation supports developments of these approaches and improve education for disaster prevention.

June, 2023
ELIMO development team
Yasunori Watanabe (Hokkaido University)

Acknowledgment

Development of ELIMO is partially supported by research grant, River Center of Hokkaido.

Bibliography

[1] Orlanski, I. (1976): A simple boundary condition for unbounded hyperbolic flows, *J. Comp. Phys.*, Vol.21, pp.251-269.

[2] Goto H., Okayasu A. and Watanabe Y. (2013), Computational Wave Dynamics, World Scientific, ISBN: 978-981-4449-70-0.

[3] Cruz E., Yokoki H., Isobe M. and Watanabe A. (1993), Annual journal of coastal engineering, JSCE, 40, pp. 46 –50.

[4] Watanabe Y., .Mitobe Y., Saruwatari A., Yamada T., Niida Y., (2012) Evolution of the 2011 Tohoku earthquake tsunami on the Pacific coast of Hokkaido, Coastal Engineering Journal, 54 (1), 1250002

[5] Okada Y. (1985): Surface deformation due to shear and tensile faults in a half-space, *Bull. Seism. Soc. Am.*, Vol. 75, pp.1135 - 1154.

[6] Tanioka Y. and Satake K. (1996): Tsunami generation by horizontal displacement of ocean bottom, *Geophysical Research Letters*, Vol. 23, No.8, pp.861-864.

[7] Hiroyasu Kawai, Makoto Stoh, Koji Kawakuchi and Katsumi Seki, Characteristics of the 2011 Tohoku tsunami waveform aquired aroud Japan by NOWPHASE equipments, Coastal Engineering Journal, 55(3), 2013.

[8] Watts, P., Grilli, S.T., M.ASCE, Tappin D.R., Fryer G.J., Tsunami generation by submarine mass failure. II: Predictive equations and cases studies, J. Waterway, Port, Coastal and Ocean Engineering, 131:6, 298 – 310, 2005

[9] Nakata K., Katsumata A., Muhari A., Submarine landslide source models consistent with multiple tsunami records of the 2018 Palu tsunami, Sulawesi, Indnesia, Earth, Planets and Space 72:44 (202).